Invited Paper

FREQUENCY-DOMAIN MULTIPLEXING FOR LARGE-SCALE BOLOMETER ARRAYS

T.M. Lanting[1],Hsiao-Mei Cho[1], John Clarke[1,2], Matt Dobbs[3], Adrian T. Lee[1,3], P.L. Richards[1,2,4], and H.G. Spieler[3]

[1]Physics Department, University of California, Berkeley, CA 94720
[2]Materials Sciences Division, Lawrence Berkeley Laboratory, Berkeley, CA 94720
[3]Physics Division, Lawrence Berkeley National Laboratory, Berkeley, CA 94720
[4]Space Sciences Laboratory, University of California, Berkeley, CA 94720

A. Smith

TRW Inc. One Space Park, Redondo Beach, CA 90278

Keywords: Bolometers, Transition-edge, multiplexer

1.ABSTRACT

We describe the development of a frequency-domain multiplexer (MUX) to read out arrays of superconducting transition-edge sensors (TES). Fabrication of large-format arrays of these sensors is becoming practical; however, reading out each sensor in the array is a major instrumental challenge that is possibly solved by frequency-domain multiplexing. Each sensor is AC biased at a different frequency, ranging from 380 kHz to 1 MHz. The sensor signal amplitude-modulates its respective AC bias frequency. An LC filter associated with each sensor suppresses Johnson noise from the other sensors. The signals are combined at a current summing node and measured by a single superconducting quantum interference device (SQUID). The individual signals from each sensor are then lock-in detected by room temperature electronics. Test chips with fully lithographed LC filters for up to 32 channels have been designed and fabricated. The capacitance and inductance values have been measured and are close to the design goals. We discuss the basic principles of frequency-domain multiplexing, the design and testing of the test chips, and the implementation of a practical system.

2.INTRODUCTION

The next generation of cosmic microwave background (CMB) observations requires a major step up in sensitivity. Wide-field cluster surveys using the Sunyaev-Zel'dovich effect and probes of the E and B-mode polarization anisotropy will become possible through large arrays of several hundred to several thousand bolometers. The development of voltage-biased superconducting transition-edge sensors with strong electro-thermal feedback is a key technology that provides well-controlled operating points and stable responsivity over large arrays.[1] A second key technology is the development of fully lithographed fabrication techniques.[2] The remaining challenge is the readout of large arrays. Transition-edge sensors typically operate at sub-Kelvin temperatures and reading out each sensor individually to room temperature would transmit too much heat across the readout wires. A possible solution is to multiplex the sensor signals in either the time-domain or the frequency-domain.[3] This paper discusses the development of a practical frequency-domain multiplexer for transition-edge sensors.

3.BASIC PRINCIPLES

An array of frequency domain multiplexed sensors may be arranged as follows. Transition-edge sensors are operated with an AC bias, with a different bias frequency applied to each sensor. When the sensor absorbs signal power, its resistance changes and modulates the signal current. This amplitude modulation transfers the signal spectrum to sidebands above and below the bias frequency. The low input impedance of the SQUID makes it the typical candidate for detecting the signal currents from the sensors. Since each sensor is operated at a different bias

Millimeter and Submillimeter Detectors for Astronomy, Thomas G. Phillips, Jonas Zmuidzinas, Editors, Proceedings of SPIE Vol. 4855 (2003) © 2003 SPIE · 0277-786X/03/$15.00

frequency, the signals corresponding to different sensors are uniquely distributed in frequency and can be combined in a common readout line. In the off-detector electronics the individual sensor signals are retrieved by a bank of frequency-selective demodulators.

Voltage Summing Circuits

The sensor signals can be combined in either a voltage or current summing configuration. First we discuss the voltage summing scheme, as originally published by Yoon et. al.[5] and shown in Fig. 1. The sensors are coupled to the summing loop by transformers, whose secondaries are connected in series and fed to an output amplifier.

To maintain constant voltage bias, the impedance presented by the transformer primary must be much smaller than the sensor resistance $\omega L_p << R$. The summing loop also provides a path for cross-talk. Any current flowing in the secondary loop will induce a voltage on the sensor side of each transformer, so the sensor drive current in a given loop will also include components from the other sensor bias generators. The attenuation of a given carrier coupled into any other sensor, in the limit $\omega L_p << R$, is given by

$$A = \frac{1}{n + \frac{Z_i}{\omega L_S}} \frac{\omega L_p}{R},$$

where n is the number of channels and Z_{in} is the amplifier input impedance. The requirement for constant bias voltage $\omega L_p << R$ also reduces the cross-talk. Isolation beyond this level for a given n requires an increase in the amplifier's input impedance, usually achieved by feedback.

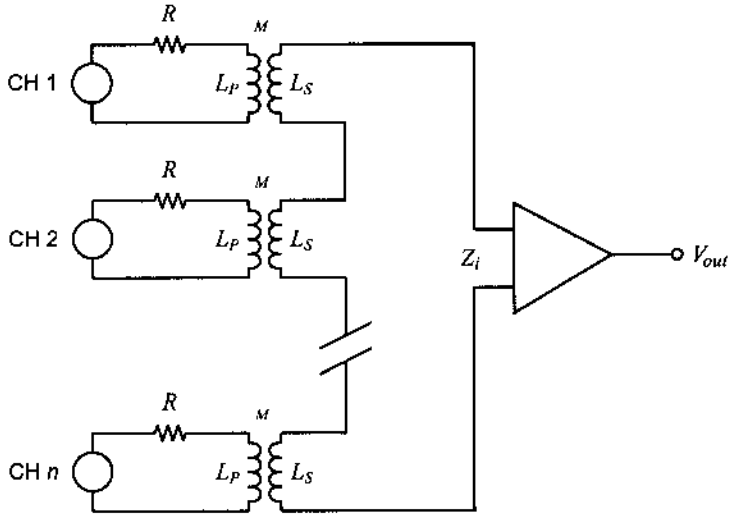

Figure 1: *Voltage summing multiplexer*

In addition to the frequency-correlated signal current, each sensor contributes a wideband Johnson noise current. As a result, superimposed on the sideband spectrum associated with each bias frequency, the Johnson noise from all other sensors will also appear. To avoid excessive noise buildup one can reduce the bandwidth of the sensor circuit by introducing frequency selective components into each sensor loop, as shown in Fig. 2. By appropriate choice of the circuit Q and the spacing between bias frequencies, the Johnson noise buildup can be kept at arbitrarily low values.

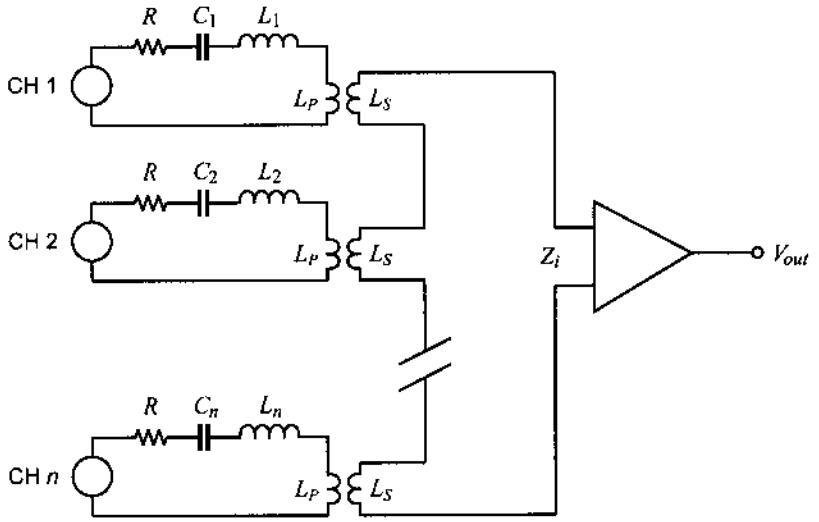

Figure 2: *Voltage summing multiplexer with tuned circuits in each sensor which limit the loop bandwidth of the sensors' Johnson noise.*

Although the circuits shown in Figs. 1 and 2 reduce the number of readout channels, they still require at least one bias wire per sensor. Introduction of the tuned circuits allows all bias frequencies to be introduced as a "comb" on a common bias line, as shown in Fig. 3. Now the tuned circuits perform double duty; they "steer" the bias drive to the appropriate sensor loop and also limit the bandwidth of the Johnson noise. Fig. 3 also shows a SQUID readout amplifier, employing series feedback to obtain a high input impedance.

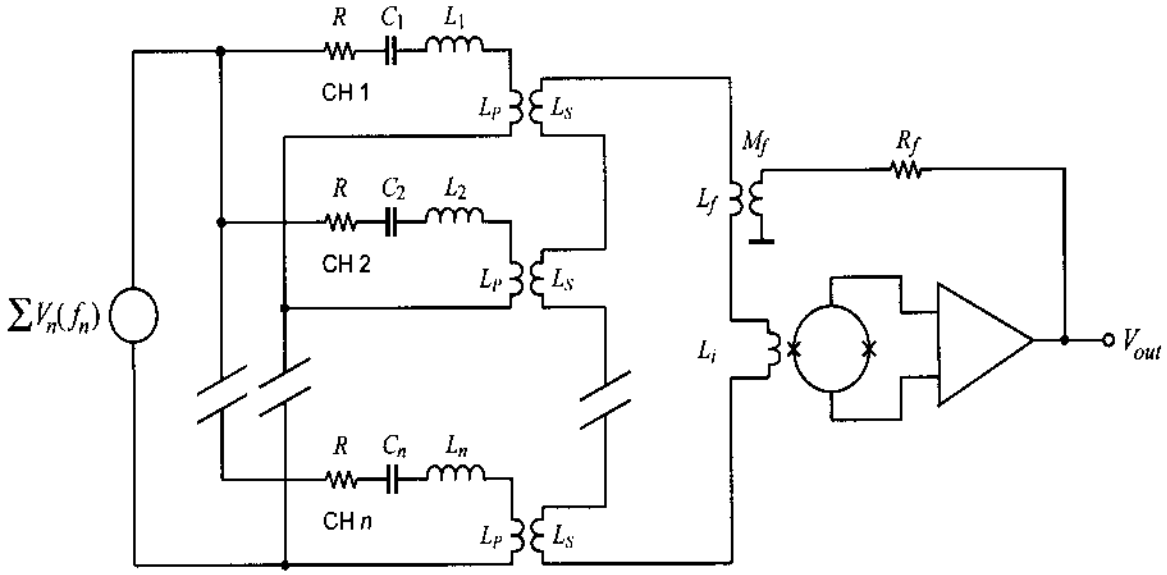

Figure 3: *Voltage summing multiplexer with common bias line.*

Current Summing Circuits

In the current summing scheme (Fig. 4), the individual sensor circuits are joined in a common current summing node at the input of the readout amplifier. To maintain constant voltage on the sensor, the input impedance of the amplifier must be much smaller than the sensor resistance, which is also required for efficient current summing. The bias cross-talk is determined by the selectivity of the tuned circuits, provided the input impedance of the amplifier is constant over the frequency range of interest. Since the full spectrum of bias frequencies is applied to all sensors, the voltage developed across the amplifier input impedance only changes the bias level of the sensors.

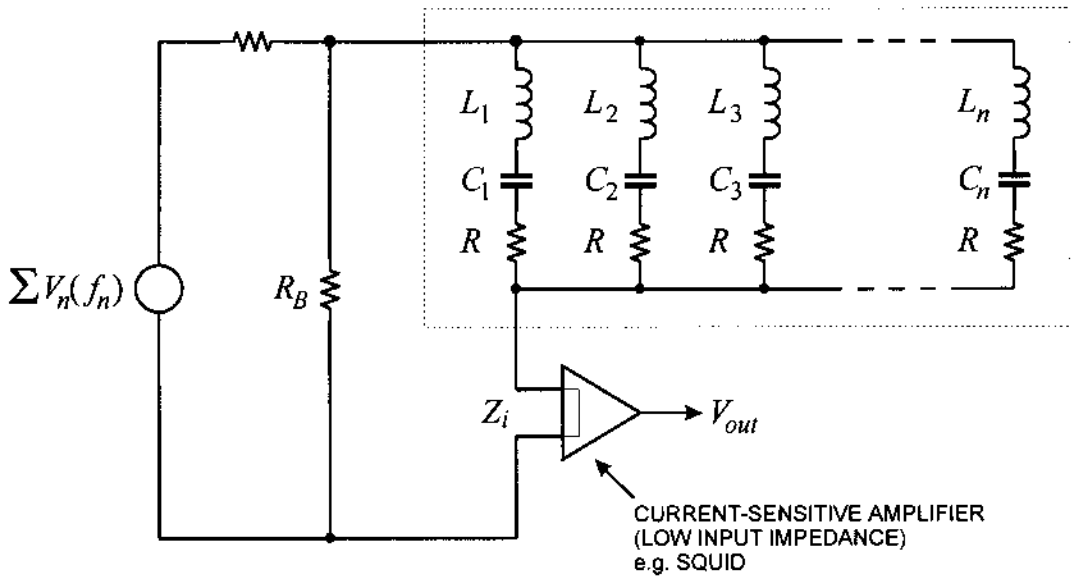

Figure 4: *Current summing multiplexer*

Apart from the complementary requirements on amplifier input impedance, the voltage and current summing schemes are fully equivalent with respect to electronic noise, dynamic range, and all other properties. The choice between the two is determined by practical considerations.

4.MUX CIRCUIT PARAMETERS

Cross Coupling of Signal and Noise

In Figs. 3 and 4 the selectivity of the individual tuned circuits determines the cross-talk between channels. For a given bias frequency the maximum current flows through the leg whose resonance matches the bias frequency. However, the finite selectivity of the other legs allows a fraction of this carrier's current to flow through them and be modulated by their respective sensors. The frequency dependence of the current flowing through the *LCR* circuit $\frac{I}{I_0} = \left(1 + Q^2\left(\Omega - \frac{1}{\Omega}\right)^2\right)^{-1/2}$, where Ω is the normalized frequency $\Omega = \omega/\omega_0$ and $\omega_0 = 1/\sqrt{LC}$. I_0 is the current at

resonance ($\Omega = 1$) and the circuit $Q = \omega_0 L / R$. At resonance the sensor is voltage-biased. Then the voltage V applied to the sensor is fixed and the bias power is $P = I_0 V$. Off-resonance, however, the voltage across the sensor depends on the fractional current I/I_0 given above and the sensor power is $P = I^2 R$. Thus, the ratio of cross-talk power is equal to the ratio of the square of the cross-talk currents, as given above. The total cross-talk is the sum of the contributions from all channels at a given frequency.

Analogously to signal cross-talk, noise from adjacent sensors is coupled into a given channel through the finite selectivity of the tuned circuits. Noise from the neighbor channels can be introduced in two ways. 1. Each sensor generates a wideband noise spectrum, shaped by the selectivity curve of the corresponding tuned circuit. Thus, noise from all sensors appears at a given bias frequency. 2. The fractional carrier current of frequency f_n flowing through the neighbor channels $f_{m \neq n}$ is modulated by the sensor noise and adds to the total noise in the sidebands associated with f_n. The relative magnitude of this contribution is determined by the bias cross-coupling, as discussed above.

Striving for acceptable levels of bias cross-coupling and noise cross-coupling between multiplexed sensors drives the selection of channel frequency spacing.

Determination of Circuit Parameters

The maximum number of channels per output line is obtained with a constant bandwidth system using the minimum allowable bandwidth, which must be greater than $f_{\max} = 1/2\pi\tau$ to ensure both constant voltage bias and electro-thermal stability, so the bandwidth is $b \approx 2/\tau$, where τ is the sensor's decay time constant. The bandwidth of a simple LC tuned circuit $b = f_0 / Q$, so constant bandwidth implies that the circuit Q is proportional to frequency. Since $Q = \omega_0 L / R_S$, this is automatically fulfilled if L is kept constant. The spacing between individual frequency "bins" is determined by the required neighbor-channel attenuation.

The circuit parameters are interrelated and determined in the following sequence:

1. The maximum Q is determined by the maximum frequency f_{max} and the required bandwidth b, $Q = f_{\max} / b$. A lower Q can be chosen at the expense of channel density.
2. The inductance is set by the adopted Q and the total resistance R in the circuit $L = RQ / 2\pi f_{\max}$.
3. The frequency spacing Δf is determined by the allowable cross-talk. All neighbors m will couple into a given channel n, so the cross-talk power to resonance power ratio is $(P/P_0)_n = \sum_{m \neq n} (I/I_0)_m^2$ and the noise ratio is $(N/N_0)_n = \sqrt{\sum_{m \neq n} (I/I_0)_m^2}$.
4. The minimum frequency is given by the thermal time constant of the sensor and by the maximum available capacitance together with the inductance calculated in step 2, $f_{\min} = 1/2\pi\sqrt{LC_{\max}}$
5. All of this together determines the number of channels per module $(f_{\max} - f_{\min})/\Delta f$.

5.BIAS AND READOUT BUSSING

As will be shown below, the number of channels that can be read out by one line is limited. In a large array the MUX "module" shown in Fig. 4 can be replicated, using the same circuitry and bias frequencies. This implies one bias oscillator per sensor. Alternatively, to reduce the number of oscillators, one can use oscillator bussing that combines all sensors using the same bias frequency, as shown in Fig. 5. However, mismatches of the resonant frequencies across the array of multiplexer modules will affect the uniformity of the bias drive level. Component matching now becomes critical for highly selective circuits. In this scheme, the finite input impedance Z_i of the current amplifier introduces bias cross-talk, KZ_{in}/R_s where the prefactor K reflects the attenuation due to the selectivity of the tuned circuits.

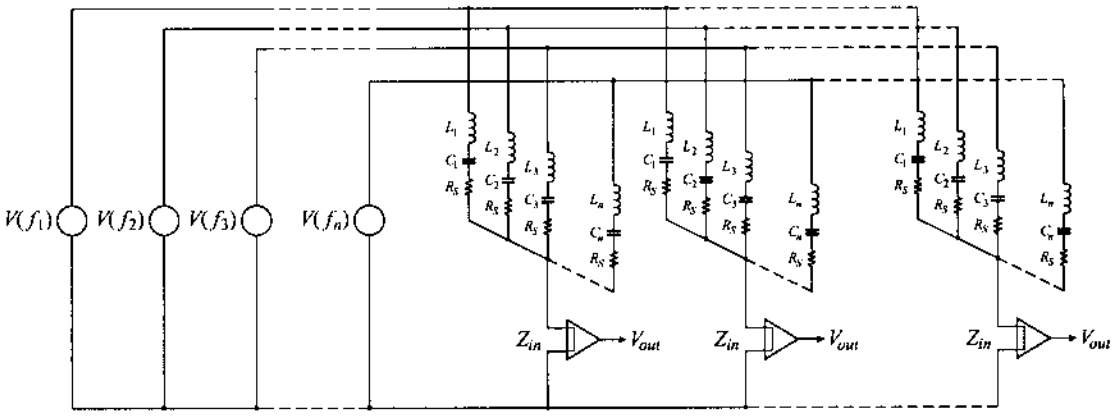

Figure 5: *Bussing by common frequency lines to gang multiple multiplexer modules*

Assume that the total array has M sensors and that each multiplexer module can combine N sensors into one readout line. Then all configurations require M/N readout lines, but differ in the number of bias lines. Fig. 1 requires M bias lines, Figs. 3 and 4 requires M/N bias lines, and Fig. 5 requires N bias lines. Thus, the total number of lines is $M/N + M$ in Fig. 1, $2M/N$ in Figs. 3 and 4, and $M/N + N$ in Fig. 5. If $M = 1024$ and $N = 32$, the number of lines is 1056, 64, and 64, respectively. Fig. 5 becomes more favorable for large M/N in terms of minimizing the combined number of bias and readout lines.

6.MAXIMUM NUMBER OF SENSORS PER MULTIPLEXER MODULE

In principle, the number of channels in a MUX module can be extended arbitrarily; increasing the number of channels increases the maximum frequency. Since the frequency spacing is constant, high frequencies provide more channel capacity than low frequencies. However, this is limited by two practical constraints, tolerances of component values and the limited dynamic range of the readout.

Mismatch of inductor and capacitor values

In practice, the inductor and capacitor values are subject to fabrication tolerances. Relative tolerances are more critical than absolute deviations. For example, if all capacitor or inductor values are high, all resonant frequencies will shift down and the spacing will remain roughly unaffected. Relative mismatches, on the other hand, can lead to a positive frequency deviation in one channel and a negative deviation in the next higher channel, so that the spacing decreases, with a corresponding increase in cross-talk. Thus, relative component mismatches require increased channel spacings at high frequencies.

Dynamic Range

The dynamic range that can be processed by the amplifier is determined by the noise floor and the maximum signal. Both voltage and current summing multiplexers can provide an ideal noise match from the sensor to the amplifier, so that the overall noise temperature is equal to the sum of the noise temperatures of the SQUID (~10 mK) and a single sensor (~100 mK). Thus, the noise floor is typically determined by the sensor noise, whereas the maximum signal that can be accepted by the SQUID depends on the SQUID feedback circuitry. Deliberately mismatching the SQUID input so that the sensor noise just overrides the SQUID noise will reduce the signal applied to the SQUID and increase the dynamic range. This will be shown below in more detail.

Maximum Acceptable Input Signal

The major problem with SQUID readouts is the limited signal range. Since the peak excursion from the baseline is limited to $\pm\Phi_0/4$ (where Φ_0 represents a quantum of magnetic flux), feedback systems are critical not just for the stabilization of the operating point, but also to extend the SQUID's dynamic range. SQUID controllers commonly use an integrator to introduce a dominant pole. This does allow the feedback loop to be stabilized against self-oscillation with a single gain adjustment, but at the expense of high-frequency dynamic range. Due to the integrator, the loop gain decreases linearly with frequency over the full frequency range, so the product of maximum input flux and frequency is constant (commonly referred to as a "slew rate limit"). In contrast, a SQUID controller has been designed with constant dynamic range $25\Phi_0$ over the full signal bandwidth of 1 MHz (corresponding to a "slew rate" of $10^8\ \Phi_0/s$).[6] However, a fundamental limit is the finite physical wire length of the feedback loop, which even with an ideal single-pole amplifier response limits the loop's gain-bandwidth product.

The SQUID's maximum allowable input signal is increased by the loop gain. For example, a maximum input signal of $25\Phi_0$ requires a loop gain $A_L \approx 25\Phi_0/(\Phi_0/4) = 100$. This loop gain also provides <1% non-linearity for signals $<\Phi_0/6$, which will be adopted as a practical signal limit. To achieve stable operation of the feedback loop the loop gain should roll off to unity at the frequency where the net phase shift is not less than 45°, i.e. one can tolerate an additional phase shift of 135° relative to the nominal 180° phase shift at low frequencies. An ideal single pole system introduces a 90° phase shift above the cutoff frequency. However, because of the finite phase velocity v_p, the physical length l of the feedback loop introduces an additional phase shift $(lf/v_p)2\pi$, so the unity gain frequency is limited to the frequency at which the propagation delay introduces the remaining 45° ($\pi/4$) phase shift, i.e. $f_0 = v_p/8l$. Thus, the gain-bandwidth product of the feedback loop $A_L f_{max} = v_p/8l$ and the upper cutoff frequency $f_{max} = v_p/8lA_L$. If $v_p = c$, a conductor length of 10 cm yields a gain-bandwidth product of 375 MHz, so for a loop gain of 100 the upper cutoff frequency is 3.75 MHz. In an insulating medium of dielectric constant ε, $v_p = c/\sqrt{\varepsilon}$, so for typical coaxial cables $v_p/c = 2/3$ and $l = 10$ cm leads to $f_{max} = c/8l\sqrt{\varepsilon}A_L = 2.5$ MHz. This limit holds for any combination of gain stages in the loop, so it does not improve for series array SQUIDs, for example. To maximize the allowable gain-bandwidth product the propagation delay must be minimized, i.e. by reducing the physical size of the amplifiers and the length of the connecting lines. A localized cold feedback loop is clearly advantageous.

We have built an implementation of this high frequency SQUID controller with minimum lead lengths in the cryostat and are currently verifying its input impedance and dynamic range across the full 1MHz bandwidth needed for our current 32-channel multiplexer design.

Carrier Nulling

Since the peak signal is dominated by the bias carrier components, one can alleviate the dynamic range requirements by suppressing the carriers. As all of the signal is in the sidebands, suppressing the carrier does not affect signal recovery. This is illustrated in Fig. 6. Suppressing the carriers 10-fold relaxes the loop gain requirements and potentially extends the bandwidth in the above example 10-fold to 25 MHz. In the simple circuit shown in Fig. 6, the practical carrier attenuation is limited, since sensor loading by intense sources will change the sensor resistance. Adaptive feedback could be used to automatically optimize carrier nulling, but we prefer to avoid carrier nulling

altogether, since it appears that we can multiplex a sufficient number of sensors per module with optimized SQUID controllers.

Estimate of Number of Channels per Readout Line

Let the sensor bias and noise currents be I_b and I_n. If the desired noise floor in the SQUID is Φ_n, the mutual inductance of the SQUID input is set to $M_i = \Phi_n / I_n$. Since the peak carrier current is $\sqrt{2}I_b$, the maximum signal $\Phi_s = n\sqrt{2}I_b M_i$ and the required loop gain $A_L = (\Phi_s/(\Phi_0/6) - 1) \approx 6n\sqrt{2}(I_b/I_n)(\Phi_n/\Phi_0)$. The loop's gain bandwidth product is limited by the length of the feedback loop $f_{max} A_L \le c/8l\sqrt{\varepsilon}$, so $f_{max} = c/\left(48nl\sqrt{2\varepsilon}(I_b/I_n)(\Phi_n/\Phi_0)\right)$. Since the number of channels $n = (f_{max} - f_{min})/\Delta f \approx f_{max}/\Delta f$, one obtains

$$f_{max} \approx \sqrt{\frac{c}{l\sqrt{\varepsilon}} \frac{\Delta f}{48\sqrt{2}(I_b/I_n)(\Phi_n/\Phi_0)}} \quad \text{and} \quad n \approx \sqrt{\frac{c}{l\sqrt{\varepsilon}} \frac{1}{48\Delta f\sqrt{2}(I_b/I_n)(\Phi_n/\Phi_0)}}.$$

A 10 cm long feedback loop with $\varepsilon = 2.25$, $\Delta f = 20$ kHz, $I_b = 1$ μA, $I_n = 10$ pA/$\sqrt{\text{Hz}}$ and $\Phi_n = 5\ \mu\Phi_0/\sqrt{\text{Hz}}$ yields $n = 54$ channels with a maximum frequency of 1.1 MHz. If carrier nulling is used with a 10-fold suppression, one obtains about 170 channels with a maximum frequency of 3.4 MHz. Note that due to the minimum frequency limit, these channel numbers must be reduced by $f_{min}/\Delta f$. Thus, for $f_{min} = 400$ kHz, the number of multiplexed channels reduces to 34 and 150, respectively.

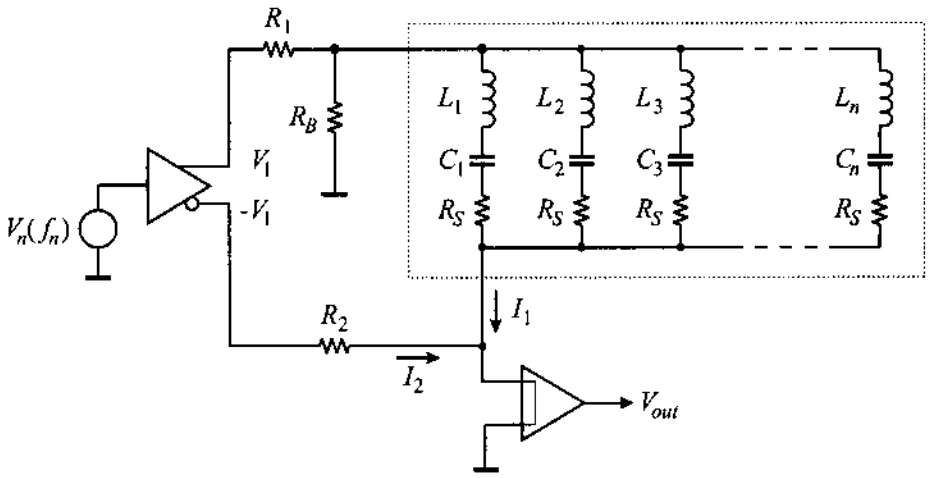

Figure 6: *The bias carrier signals can be suppressed to reduce dynamic range requirements.*

7.CURRENT MUX DESIGN

We have designed a 32-channel current-summing multiplexer using the configuration shown in Fig. 4. Each sensor circuit is bandwidth-limited by a series LC (inductor and capacitor) combination. The fabrication was performed by TRW[7]. The frequency range is from 380 kHz to 1 MHz with a nominal channel spacing of 20 kHz. For this test the multiplexer was subdivided into four 8-channel chips, whose resonant frequencies are interleaved so that within one chip the frequency spacing is 4 times the nominal spacing. The 8-channel chips can be used individually with 4-fold channel spacing or connected in parallel to form either a 16-channel or a full 32-channel multiplexer. Bond pads are provided to allow measurement of individual inductors and capacitors. Fig. 7 shows the layout of one chip; the die size is 1 cm. The capacitors use Nb_2O_5 dielectric formed by anodization of Nb. This yields a capacitance of 3 nF/mm^2 with very good uniformity. The inductors are implemented as square spirals. Spiral inductors have a large fringing field, so to reduce the sensitivity of the inductance to nearby objects, the inductors utilize a "transformer"

geometry as used in SQUIDs, where the inductor spiral is tightly coupled to a square washer slit at one side.[8] The inductors all have the same value of 39.8 μH and with a winding pitch of 4 μm are 2.2 mm on a side. The capacitances range from 640 pF to 4.4 nF. At a frequency spacing of 20 kHz and a maximum Q of 500 (at 1000 kHz) the calculated noise degradation due to all neighbor channels is 9% and bias cross-talk due to the attenuation of the tuned circuits is less than 0.8%. For a given sensor the cross-talk is the sum of the currents at all undesired frequencies divided by the current at the resonance frequency.

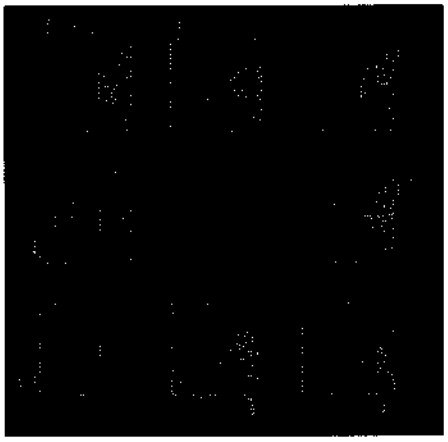

Figure 7: *Layout of 8-channel MUX chip. The eight inductors surround a central capacitor core.*

The devices have been fabricated successfully and the resonant frequencies of the circuits have been measured. We did not observe significant relative shifts in resonance frequency with respect to the design goals, although we did measure an absolute shift upwards in resonance frequency for all LC circuits of approximately 7%. This absolute shift is much less critical, however, since it does not affect channel spacing, and therefore bias and noise cross-coupling between channels are maintained.

8.READOUT ELECTRONICS

The frequency-domain multiplexer reverts to full parallelism at the signal recovery stage, i.e. after current amplification by the SQUID. We have adopted a fully analog demodulation system, shown in Fig. 8. In principle, a digital signal processor (DSP) could be used to retrieve all of the signals. However, at the high frequencies (~1MHz) we are using, this is presently not practical, although we are considering this option for future arrays.

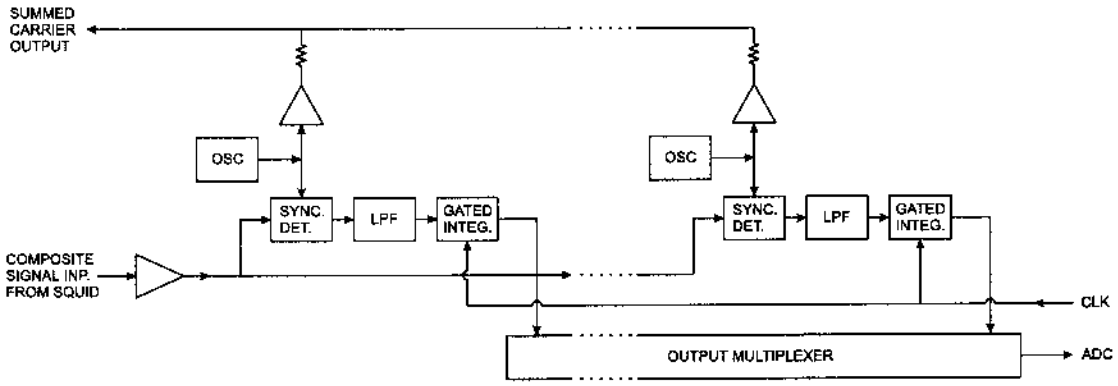

Figure 8: *Off-detector readout electronics*

The composite signal stream is fed to a bank of phase-synchronous demodulators. The same carrier oscillators used to bias the sensors are used for demodulation. Thus, to first order, oscillator sideband noise cancels out. Direct digital synthesis (DDS) oscillators provide both frequency and phase adjustability. The output of the synchronous detector feeds a low-pass filter and then a gated integrator. These integrators are all gated by the same clock, to ensure that all measurements in the array cover the same time intervals. The outputs of the gated integrators are multiplexed to a multichannel PC-based analog to digital converter (ADC) with differential inputs to provide common-mode isolation. Digitization occurs within less time than the integration interval, so there is no dead time. Our current design has 32 channels per multiplex module, so 1000 channels require about 30 modules, all of which are identical. All circuit functions can be performed by economical standard ICs.

9.STATUS OF MULTIPLEXER IMPLEMENTATION

Although one might read out several hundred sensors with one readout line, this introduces a significant single-point failure mode, so 30 – 50 sensors per readout line appears to be a reasonable choice. Detailed designs are underway for arrays of 300 – 3000 bolometers in next-generation CMB experiments. Use of SQUIDs as readout amplifiers necessitates carefully optimized feedback loops to achieve the required dynamic range and bandwidth. As described in this paper, we have designed and built a high-frequency constant gain SQUID controller and a prototype 32-channel MUX with on-chip inductors and capacitors that have the desired resonant frequencies. Component tests are nearing completion and we are preparing to multiplex transition-edge sensors.

Frequency domain multiplexing has also been demonstrated with x-ray sensors. The circuit in Fig. 2 has been used to multiplex x-ray TES devices with no degradation in resolution.[9]

10.SUMMARY

Frequency-domain multiplexers provide a practical method of reading out large arrays of superconducting transition-edge sensors. They provide continuous readout with no switching transients. Practical designs have been developed and are now being tested and evaluated for use in large-scale CMB experiments.

This work was supported by NSF Grant AST-00-96933, NASA Grant No. NAG5-11422 and by the Director, Office of Energy Research, Office of Basic Energy Science, Materials Sciences Division of the U. S. DOE under contract number DE-AC03-76SF00098. M.D. and H.S. are supported by the Director, Office of Science, Office of High Energy and Nuclear Physics, of the U.S. DOE under Contract No. DE-AC03-76SF00098.

1. S.-H. Lee, *et al.*, A Voltage-Biased Superconducting Transition Edge Bolometer with Strong Electro- Thermal Feedback Operated at 370 mK, Applied Optics **37**, 3391 (1998).
2. Gildemeister, J.M., Lee, A.T., and Richards, P.L., Monolithic Arrays of Absorber-Coupled Voltage-Biased Superconducting Bolometers, Appl. Phys. Lett. 77, 4040 (2000).
3. Irwin, K.D. SQUID multiplexers for transition-edge sensors. Physica C, vol.368, (no.1-4), Elsevier, 1 March 2002. p.203-10.
4. Chervenak, J.A., *et al.*, Superconducting Multiplexer for Arrays of Transition Edge Sensors, Appl. Phys. Lett. **74**, 4043-4045 (1999).
5. Yoon, J., *et al.*, Single Superconducting Quantum Interference Device Multiplexer for Arrays of Low-Temperature Sensors, Appl. Phys. Lett. **78**, 371 (2001)
6. Helmuth Spieler, internal note
7. TRW Inc., One Space Park, Redondo Beach, CA 90278
8. J.M. Jaycox and M.B. Ketchen, Planar Coupling Scheme for Ultra-Low Noise DC SQUIDs, IEEE Trans. on Magnetics **MAG-17/1** (1981) 400-403
9. M.F. Cunningham, J.N. Ullom, T. Miyazaki, S.E. Labov, John Clarke, T.M. Lanting, Adrian T. Lee, P.L. Richards, Jongsoo Yoon, and H. Spieler, High-Resolution Operation of Frequency-Multiplexed Transition-Edge Photon Sensors, accepted by Applied Physics Letters.